Microcomb design and fabrication for high accuracy optical assembly

Carl G. Chen,[a] Ralf K. Heilmann, Paul T. Konkola, Olivier Mongrard, Glen P. Monnelly, and Mark L. Schattenburg
Massachusetts Institute of Technology, Cambridge, Massachusetts 02139

(Received 1 June 2000; accepted 25 July 2000)

There are two popular optic designs for x-ray space telescopes: the traditional monolithic design, which has demonstrated subarcsecond resolution but at enormous weight and cost per collecting area, and the foil design, which has achieved far greater collecting area per weight and cost, but with resolution limited to the arcminute level, in part due to foil assembly inaccuracy. In this article, we present the design and the fabrication of a novel micromechanical device, the so-called microcomb, which is used to assemble high-accuracy foil x-ray optics. To achieve submicron foil alignment accuracy, two types of microcombs have been fabricated via microelectromechanical systems technology. Reference combs provide highly accurate single-point contacts against which foils are registered, and spring combs provide the mechanical actuation needed to properly position and shape the foils. Briefly, we introduce some basic concepts regarding grazing-incidence x-ray optics. We then present a theoretical model that has given rise to the unique shape of the spring microcomb. Finally, the fabrication process used to produce the microcombs is discussed. [S0734-211X(00)01606-1]

I. INTRODUCTION

Astronomical x rays cover the wavelength range from approximately 0.01 to 10 nm, corresponding to photon energies from 120 eV to 120 keV. At x-ray frequencies, the behavior of a material's index of refraction $n(\omega)$ is described by

$$n(\omega)=1-\delta(\omega)+i\beta(\omega), \tag{1}$$

where δ and β are real functions of the angular frequency ω and have magnitude 10^{-3} or less. The real part of Eq. (1) describes the phase velocity of light in the medium, which is slightly larger than c, the speed of light in vacuum, while the imaginary part gives rise to absorption. Because x rays are strongly absorbed by most materials including air, x-ray observations must be conducted above Earth's atmosphere. Heavy extinction also explains why x-ray refractive optics are difficult to implement.

Equation (1), together with the Maxwell equations, determine the x-ray reflection and refraction characteristics of a vacuum–material interface.[1] Broadband normal-incidence x-ray reflective optics are effectively ruled out. On the other hand, for radiation incident at grazing angles, total external reflection arises where nearly 100% of the incident radiation is reflected for θ smaller than a certain critical angle $\theta_c = \sqrt{2\delta}$ [Fig. 1(a)].

For years, astronomers have exploited the properties of total external reflection to build grazing-incidence x-ray telescopes. Figures 1(b) and 1(c) show schematics of the popular Wolter type I telescope.[2,3] Optimal collecting area is ensured by nesting multiple confocal mirror shells.

II. MICROCOMB

Traditionally, each mirror onboard telescopes such as the Chandra X-ray Observatory has been fabricated out of a single substrate block.[4] The monolithic design is capable of subarcsecond resolution,[5] but yields low collecting-area-to-weight ratio. An alternative is the so-called segmented foil design,[6] which employs thousands of lightweight segmented mirror foils, each a few hundred microns in thickness, to focus x rays (Fig. 2). Despite having overwhelming advantages over the monolithic design in terms of cost, weight, and collecting area, foil telescopes have thus far demonstrated only arcminute-level imaging. A major deterrent to better resolution is the lack of properly engineered foil assembly and alignment tools. Figure 2(c) is a close-up scanning electron microscopy (SEM) image of one of the previous generation foil alignment/mounting bars visible as radial spokes in Fig. 2(a). The roughness of the electrical-discharge machined (EDM) grooves is clearly visible. Foils aligned and mounted with these coarse bars are prone to positioning inaccuracy, measured at tens of microns.

Future x-ray telescope missions with arcsecond angular resolution will require submicron foil positioning accuracy.[7] We have devised a novel foil alignment scheme that separates alignment from assembly and utilizes microfabricated alignment bars, the so-called microcombs. Foils are first aligned with the microcombs and then bonded to coarse EDM bars.[8] As illustrated in Fig. 3(a), two types of comb structures have been designed. The reference comb makes contact with a foil at a single reference point [A in Fig. 3(a)]. The spring comb has a built-in microspring actuation mechanism, which when compressed, generates a minute force that steadfastly pushes a foil to its final position against the reference comb. Figure 3(b) shows schematically how foils are aligned. Actual telescope combs would feature variable comb tooth spacing appropriate for Wolter optics.

Prototype microcombs have been fabricated from 100-mm-diam double-side-polished silicon wafers, with a thickness of about 380 μm (Fig. 4). The measured comb slot

[a]Electronic mail: gangchen@mit.edu

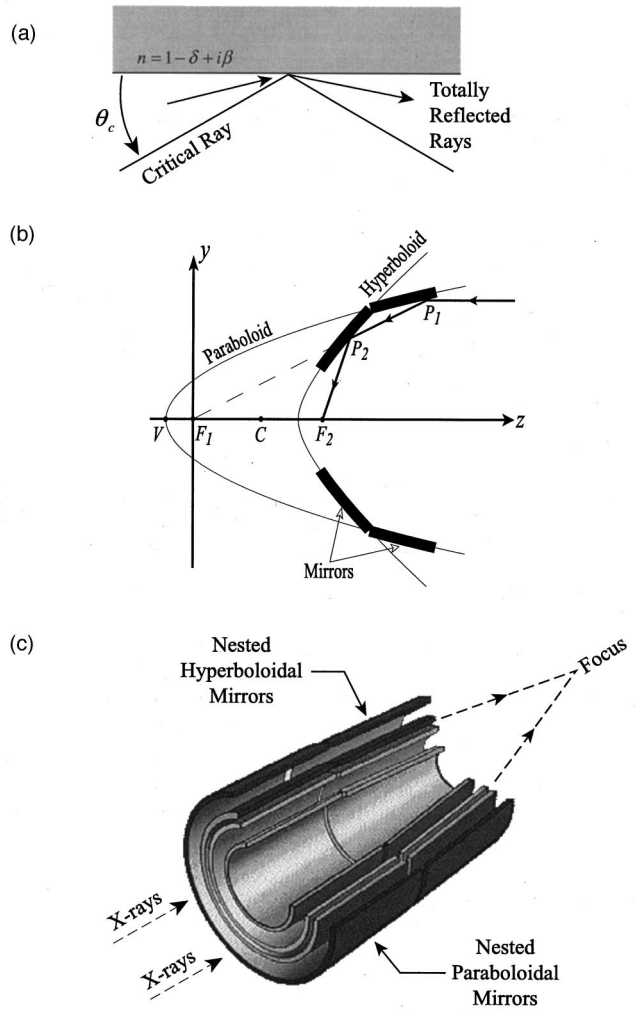

FIG. 1. (a) Principle of grazing incidence radiation and total external reflection. Note that by convention, incident angle is measured with respect to the surface, not to the surface normal. (b) 2D cross-sectional schematic of a Wolter type I telescope. (c) 3D schematic of a nested Wolter type I telescope.

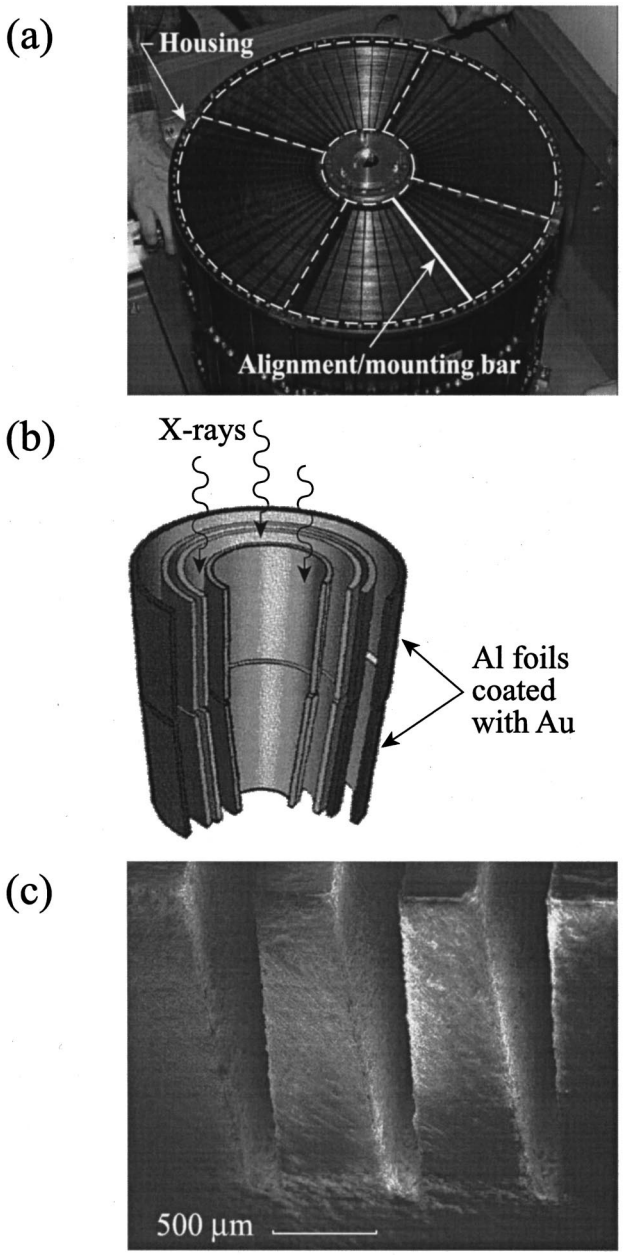

FIG. 2. (a) Mirror module from the Astro-E Satellite. The housing is 40 cm in diameter and consists four segmented quadrants, outlined by dashed lines. Each quadrant contains 175 pairs of aluminum foils, aligned and mounted by radial electrical-discharge machined (EDM) bars, one of which is outlined in white. (b) Schematic showing the foil layout inside the Astro-E mirror module. (c) SEM image of the EDM grooves in an alignment/mounting bar shown in (a).

spacing tolerance is 1 μm or less, and the average surface roughness is approximately 0.2 μm. Initial tests with the microcombs have demonstrated subarcsecond foil assembly reproducibility, and ± 10 microradians (2 arcsec) slot-to-slot repeatability.[9] Ultimately, foil alignment accuracy on the order of a few tens of nanometers should be possible with the microcomb assembly scheme, which will make diffraction-limited resolution a reality.

It should be noted that even though our prototype combs are made for x-ray telescopes, they can be easily modified to suit a wide variety of applications that call for submicron parts' placement.

III. SPRING MICROCOMB DESIGN

Since the overall length l of the spring is much greater than its width h, it can be analytically modeled as a flexible cantilever, with one end fixed and the other end receiving a load F [Fig. 5(a)]. Two well-known equations govern the state of the cantilever.[10] They are

$$\frac{F}{\delta} = \frac{Eh^3 t}{4l^3}, \tag{2a}$$

$$\frac{\sigma}{F} = 6\frac{l}{th^2}, \tag{2b}$$

where δ is the displacement of the cantilever, E is the Young's modulus for silicon, t is the thickness of the wafer, and σ is the stress felt at the base of the cantilever.

The minimum load $F_{\min}$ is a sum of three terms,

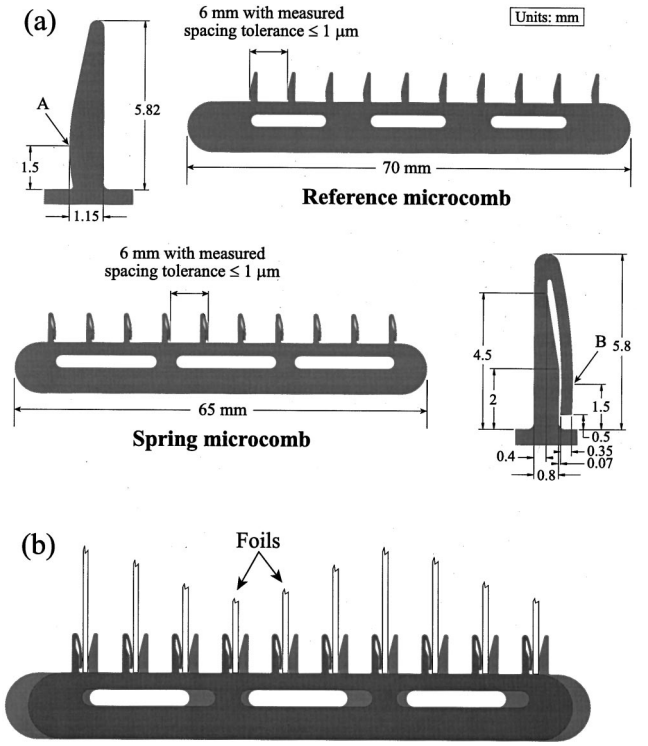

FIG. 3. (a) Prototype reference and spring microcomb designs. (b) Foil alignment scheme using the microcombs.

$$F_{\text{min}} = F_{\text{figure}} + F_{\text{bending}} + F_{\text{friction}}. \tag{3}$$

The term F_{figure} represents a force imparted to the spring due to a foil's intrinsic figuring error, F_{bending} is due to any slight bending of the foil that we desire to impart, and F_{friction} is due to the fact that the bottom of the foil, resting on the microcomb, gives frictional resistance when the foil is pushed. The cantilever displacement δ must accommodate not only an ''equilibrium'' displacement, $\delta^* = \delta^*(F_{\text{min}})$, but also the maximum foil-to-foil thickness variation d_{max}.

Knowing both F_{min} and d_{max}, we can generate, for each stress σ_{max} input, a corresponding spring length l vs width h curve [Fig. 5(b)]. For chosen $\sigma_{\text{max}} = 300$ MPa, which is half the maximum bending stress sustainable by silicon, the above analysis yields $l = 2.5$ mm and $h = 0.26$ mm. Subsequent ANSYS finite-element modeling modified the values to $l = 3.5$ mm and $h = 0.35$ mm, which gave an ANSYS stress of 288 MPa.

IV. MICROCOMB FABRICATION

The microcombs are fabricated with microelectromechanical systems (MEMS) technology. Combs are first patterned onto a 100-mm-diam double-side-polished silicon wafer via contact lithography, and then etched through the wafer with time multiplexed deep reactive ion etch (TMDRIE). The overall fabrication process is schematically presented in Fig. 6.

Unlike conventional reactive ion etching (RIE), which employs a single plasma cycle that simultaneously etches and passivates, TMDRIE[11] alternates sequentially between two cycles, one etches and the other passivates [Fig. 7(a)]. The etch and passivation gases that we chose to use are SF_6

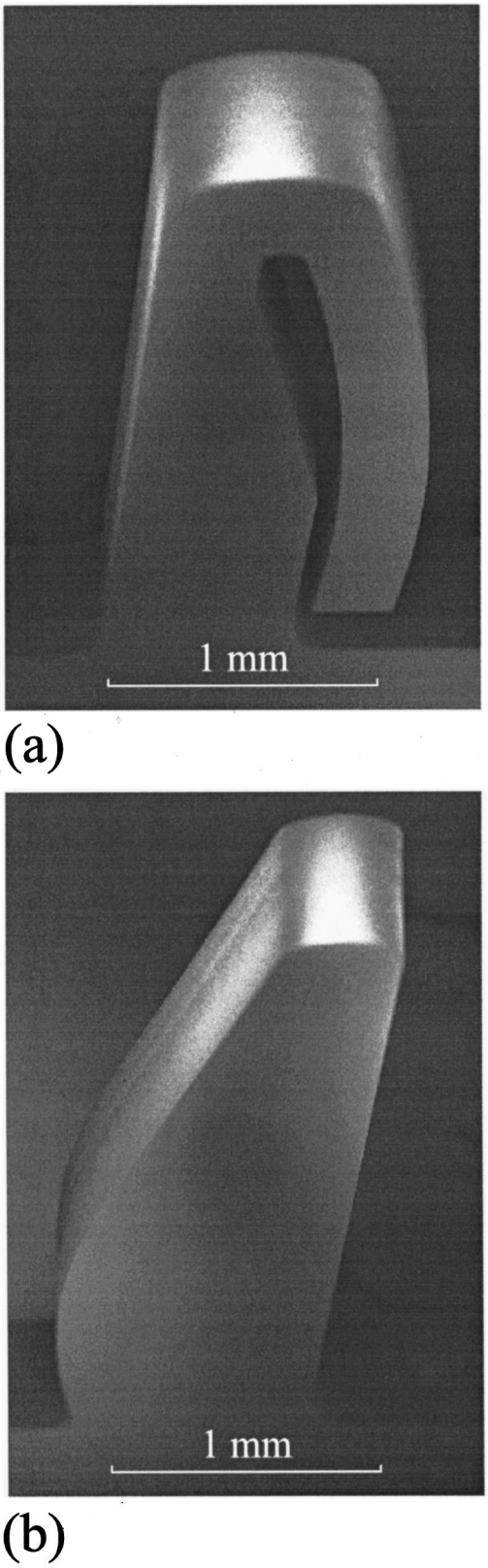

FIG. 4. (a) SEM image of the fabricated spring microcomb. (b) SEM image of the fabricated reference microcomb.

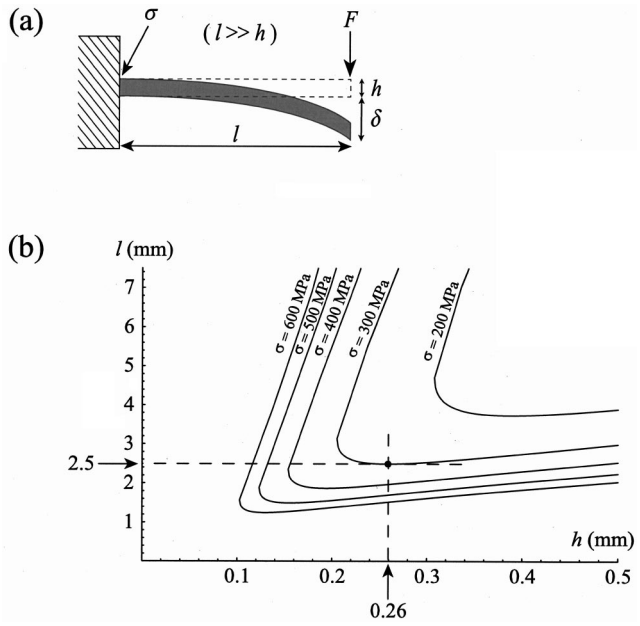

FIG. 5. (a) Spring microcomb modeled as a cantilever. (b) Spring length l vs width h curves, calculated for $F_{min}=0.18$ N, $d_{max}=20$ μm, and five different stress values.

and C_4F_8, respectively. The sequential alternation between the etching and passivation cycles leaves vertical striation marks, or scalloping, on the trench sidewalls [Fig. 7(b)]. It is this scalloped pattern that gives the finished microcombs a surface roughness of approximately 0.2 μm.

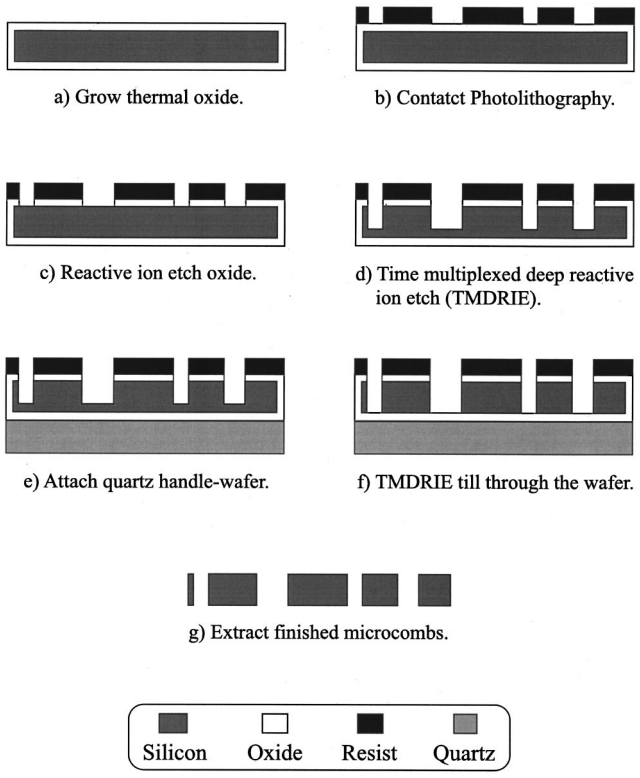

FIG. 6. Microcomb fabrication process overview.

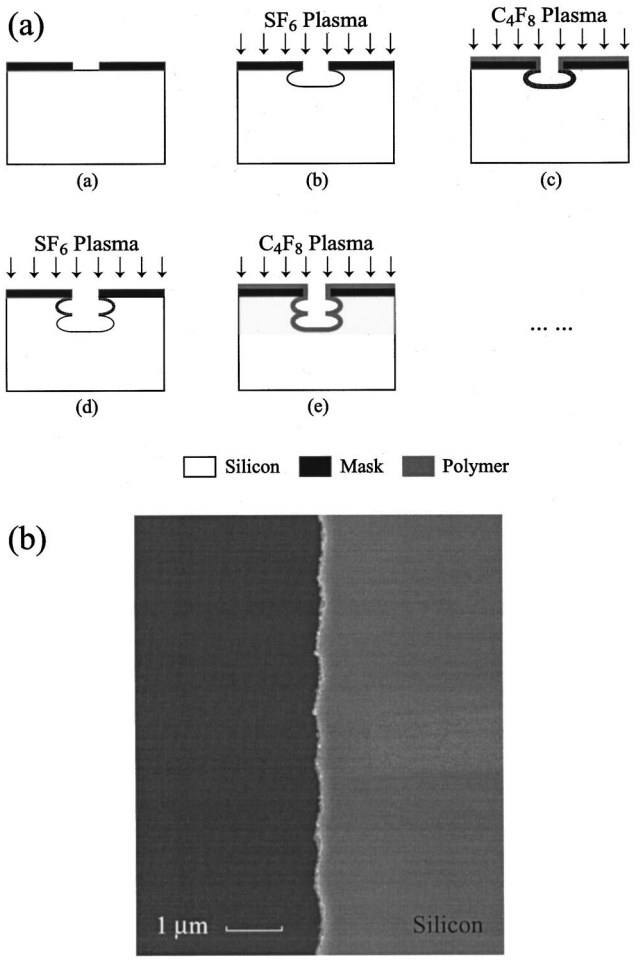

FIG. 7. (a) Time multiplexed deep reactive ion etch process (TMDRIE). (b) ''Scalloping'' caused by TMDRIE.

The plasma is generated by an inductively coupled plasma (ICP) etcher.[12] ICP is a cost effective and flexible excitation technique to create low pressure and high ion density plasmas, a necessity for producing high-aspect-ratio MEMS structures.[13] During etching [step (d) in Fig. 6], the wafer is cooled from the back by helium gas. The low temperature (40 °C at the top surface) enables the use of photoresist as a soft mask for etching silicon. However, to prevent plasma contamination due to helium leakage into the chamber, we attach a quartz handle wafer to the backside of the device wafer, at a time when etch through is imminent [step (e)]. The attachment is done with photoresist in a target pattern to allow channels for resist outgasing.

Due to feature size variations and a slight noncircular symmetry in the ICP coupling coil itself, silicon etch rates at points across the wafer surface are slightly different. The nonuniformity is on the order of 4% for our process. The time period between the initial and final etch through is near a few tens of minutes, during which, etching agents, stopped by the quartz handle wafer, will be redirected through the crevices between the device and handle wafers, and start to attack the silicon from the backside, resulting in significant feature loss. As a solution, we thermally grow an oxide layer

TABLE I. Key parameters obtained after a 1 h etch.

Silicon etch rate	2.5 μm/min
Selectivity to photoresist	90:1
Selectivity to oxide	290:1
Sidewall profile	0.8° undercut
Etch uniformity across the wafer	4%

of thickness 1.5μm on the device wafer [step (a) in Fig. 6], which serves as a stop during etch overruns [step (f)].

Table I summarizes key etch parameters obtained after a 1 h etch.

V. CONCLUSIONS

We have described a novel foil alignment scheme that utilizes micromachined devices called microcombs. The scheme is capable of subarcsecond foil placement. An analytical design in which the spring microcomb is modeled as a flexible cantilever is described. Both the reference and spring microcombs have been successfully prototyped with MEMS technology. Specifically, an ICP etcher with a TMDRIE process has been used to etch the combs through a 100-mm-diam silicon wafer. The characters of ICP combined with those of TMDRIE produced fast etch rate (>2 μm/min) and good anisotropic profile control (0.8° undercut). The finished microcombs have been measured to a relative spacing tolerance of <1 μm, and an average surface roughness of approximately 0.2 μm.

ACKNOWLEDGMENTS

The authors gratefully acknowledge the technical support of James Carter, James Daley, Robert Fleming, Wendy Gu, and Edward Murphy, and informative discussions with Lester Cohen, Vicky Diadiuk, Ravi Khanna, and Steven Nagle. Staff and facility support from the Microsystems Technology Laboratories, the NanoStructures Laboratory and the Space Nanotechnology Laboratory are also appreciated. This work was sponsored by NASA under Grant Nos. NAG5-5105, NAG5-5271, and NCC5-330.

[1]D. Attwood, in *Soft X Rays and Extreme Ultraviolet Radiation: Principles and Applications* (Cambridge University Press, Cambridge, 1999).
[2]H. Wolter, Ann. Phys. **10**, 94 (1952).
[3]H. Wolter, Ann. Phys. **10**, 286 (1952).
[4]P. B. Reid, T. E. Gordon, and M. B. Magida, Proc. SPIE **1618**, 45 (1992).
[5]M. C. Weisskopf and S. L. O'dell, Proc. SPIE **3113**, 2 (1997).
[6]P. J. Serlemitsos and Y. Soong, Astrophys. Space Sci. **239**, 177 (1996).
[7]R. Petre *et al.*, Proc. SPIE **3766**, 11 (1999).
[8]C. G. Chen, S. M. dissertation, Massachusetts Institute of Technology, Department of Electrical Engineering, 2000.
[9]G. Monnelly *et al.*, Proc. SPIE (to be published).
[10]J. E. Shigley and C. R. Mischke, in *Mechanical Engineering Design*, 5th ed. (McGraw–Hill, New York, 1989).
[11]J. Bhardwaj, H. Ashraf, and A. McQuarrie, in Proceedings of the Third International Symposium on Microstructures and Microfabricated Systems, edited by P. J. Hesketh, G. Barna, and H. G. Hughes, 1977 (unpublished), pp. 118–130.
[12]A. A. Ayón *et al.*, J. Electrochem. Soc. **146**, 339 (1999).
[13]J. K. Bhardwaj and H. Ashraf, Proc. SPIE **2639**, 224 (1995).